Carbon Monoxide Induced Decomposition of the Active Site [Ni−4Fe−5S] Cluster of CO Dehydrogenase

Holger Dobbek,*,[†] Vitali Svetlitchnyi,[‡] Jago Liss,[‡] and Ortwin Meyer[‡,§]

Contribution from the Laboratorium für Proteinkristallographie, Lehrstuhl für Mikrobiologie, and Bayreuther Zentrum für molekulare Biowissenschaften, Universität Bayreuth, Bayreuth, Germany

Received August 6, 2003; E-mail: Holger.Dobbek@uni-bayreuth.de

Abstract: During the past two years, crystal structures of Cu- and Mo-containing carbon monoxide dehydrogenases (CODHs) and Ni- and Fe-containing CODHs have been reported. The active site of CODHs from anaerobic bacteria (cluster C) is composed of Ni, Fe, and S for which crystallographic studies of the enzymes from *Carboxydothermus hydrogenoformans*, *Rhodospirillum rubrum*, and *Moorella thermoacetica* revealed structural similarities in the overall protein fold but showed substantial differences in the essential Ni coordination environment. The [Ni−4Fe−5S] cluster C in the fully catalytically competent dithionite-reduced CODH II from *C. hydrogenoformans* (CODHII$_{Ch}$) at 1.6 Å resolution contains a characteristic μ_2-sulfido ligand between Ni and Fe1, resulting in a square-planar ligand arrangement with four S-ligands at the Ni ion. In contrast, the [Ni−4Fe−4S] clusters C in CO-treated CODH from *R. rubrum* resolved at 2.8 Å and in CO-treated acetyl-CoA synthase/CODH complex from *M. thermoacetica* at 2.2 and 1.9 Å resolution, respectively, do not contain the μ_2-sulfido ligand between Ni and Fe1 and display dissimilar geometries at the Ni ion. The [Ni−4Fe−4S] cluster is composed of a cubane [Ni−3Fe−4S] cluster linked to a mononuclear Fe site. The described coordination geometries of the Ni ion in the [Ni−4Fe−4S] cluster of *R. rubrum* and *M. thermoacetica* deviate from the square-planar ligand geometry in the [Ni−4Fe−5S] cluster C of CODHII$_{Ch}$. In addition, the latter was converted into a [Ni−4Fe−4S] cluster under specific conditions. The objective of this study was to elucidate the relationship between the structure of cluster C in CODHII$_{Ch}$ and the functionality of the protein. We have determined the CO oxidation activity of CODHII$_{Ch}$ under different conditions of crystallization, prepared crystals of the enzyme in the presence of dithiothreitol or dithionite as reducing agents under an atmosphere of N$_2$ or CO, and solved the corresponding structures at 1.1 to 1.6 Å resolutions. Fully active CODHII$_{Ch}$ obtained after incubation of the enzyme with dithionite under N$_2$ revealed the [Ni−4Fe−5S] cluster. Short treatment of the enzyme with CO in the presence of dithiothreitol resulted in a catalytically competent CODHII$_{Ch}$ with a CO-reduced [Ni−4Fe−5S] cluster, but a prolonged treatment with CO caused the loss of CO-oxidizing activity and revealed a [Ni−4Fe−4S] cluster, which did not contain a μ_2-S. These data suggest that the [Ni−4Fe−4S] cluster of CODHII$_{Ch}$ is an inactivated decomposition product originating from the [Ni−4Fe−5S] cluster.

Introduction

The utilization of CO is a central metabolic feature of several aerobic and anaerobic microorganisms.[1,2] Carbon monoxide dehydrogenases (CODHs), the enzymes responsible for CO-metabolism, all catalyze formally the same reaction: $CO + H_2O \leftrightarrow CO_2 + 2e^- + 2H^+$.[3−5] Two principal types of CODHs can be defined according to their metal composition and distribution: Mo- and Cu-containing CODHs employed by aerobic carboxidotrophic bacteria such as *Oligotropha carboxidovorans*[6,7] and Ni- and Fe-containing CODHs functioning in diverse groups of anaerobic bacteria and archaea.[2,8−10] The anaerobic thermophilic hydrogenogenic eubacterium *Carboxydothermus hydrogenoformans*[11] grows chemolithoautotrophically on CO as a sole source of energy and carbon. It couples the oxidation of CO to the reduction of protons, which serve as the ultimate intracellular electron acceptor.[11,12] The oxidation of CO in *C. hydrogenoformans* is catalyzed by two monofunctional NiFe CODHs (CODH I and CODH II),[12] while a third CODH (CODH III) is

† Laboratorium für Proteinkristallographie.
‡ Lehrstuhl für Mikrobiologie.
§ Bayreuther Zentrum für molekulare Biowissenschaften.

(1) Moersdorf, G.; Frunzke, K.; Gadkari, D.; Meyer, O. *Biodegradation* **1992**, *3*, 61−82.
(2) Ferry, J. G. *Ann. Rev. Microbiol.* **1995**, *49*, 305−333.
(3) Lindahl, P. A. *Biochemistry* **2002**, *41*, 2097−2105.
(4) Meyer, O.; Gremer, L.; Ferner, R.; Ferner, M.; Dobbek, H.; Gnida, M.; Meyer-Klaucke, W.; Huber, R. *Biol. Chem.* **2000**, *381*, 865−876.
(5) Ragsdale, S. W.; Kumar, M. *Chem. Rev.* **1996**, *96*, 2515−2539.
(6) Dobbek, H.; Gremer, L.; Kiefersauer, R.; Huber, R.; Meyer, O. *Proc. Natl. Acad. Sci. U.S.A.* **2002**, *99*, 15971−15976.
(7) Gnida, M.; Ferner, R.; Gremer, L.; Meyer, O.; Meyer-Klaucke, W. *Biochemistry* **2003**, *42*, 222−230.
(8) Dobbek, H.; Svetlitchnyi, V.; Gremer, L.; Huber, R.; Meyer, O. *Science* **2001**, *293*, 1281−1285.
(9) Lindahl, P. A. *Biochemistry* **2002**, *41*, 2097−2105.
(10) Drennan, C. L.; Peters, J. W. *Curr. Opin. Struct. Biol.* **2003**, *13*, 220−226.
(11) Svetlitchnyi, V. A.; Sokolova, T. G.; Gerhardt, M.; Ringpfeil, N. A.; Kostrikina, N. A.; Zavarzin, G. A. *Syst. Appl. Microbiol.* **1991**, *14*, 254−260.
(12) Svetlitchnyi, V.; Peschel, C.; Acker, G.; Meyer, O. *J. Bacteriol.* **2001**, *183*, 5134−5144.
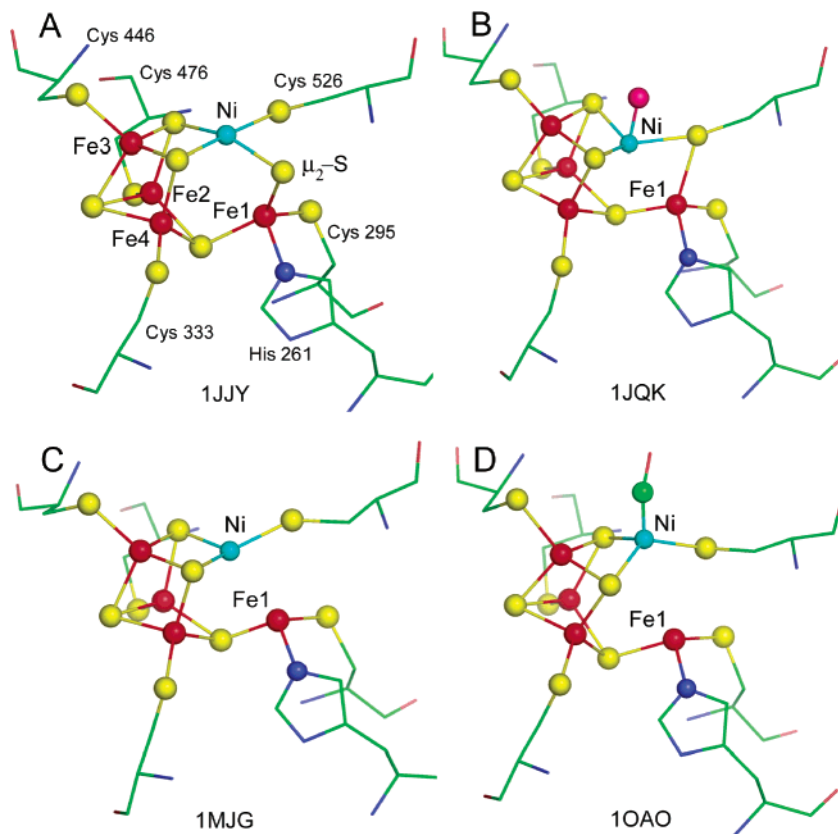
Figure 1. Four models, which have been proposed for cluster C. (A) The [Ni−4Fe−5S] cluster, found in CODHII$_{Ch}$ at a resolution of 1.63 Å.[8] (B) The 2.8 Å structure of cluster C in the CODH$_{Rr}$, interpreted as an [Ni−4Fe−4S] cluster. An additional ligand of unknown nature has been modeled in the apical coordination site at the Ni ion.[14] (C) Cluster C in the 2.2 Å structure of CODH$_{Mt}$.[17] (D) Cluster C in the 1.9 Å structure of CODH$_{Mt}$ with a CO ligand modeled in the apical coordination site of Ni.[16] In the 1.9 Å structure, apparent disorder of cluster C has been observed of which only the positions with higher occupancy have been depicted here. The proposed structures are listed according to the order of their publication. The PDB-entry codes for the protein structure coordinates are shown below the individual pictures. Figures 1 and 3−6 have been created using the program PyMol.[18]

found in a complex with an acetyl-CoA synthase involved in the autotrophic carbon assimilation.[13] Fully catalytically competent CODH II from *C. hydrogenoformans* (CODHII$_{Ch}$) was crystallized under an atmosphere of N$_2$ in the presence of dithionite, and its structure has been solved at 1.63 Å resolution.[8] The crystal structure shows a mushroom-shaped homodimeric protein with five metal clusters. Each subunit contains an asymmetrical [Ni−4Fe−5S] cluster C along with a conventional cubane-type [4Fe−4S] cluster B. An additional [4Fe−4S] cluster D is bound at the subunit interface of the homodimer. Cluster C is the active site of CO oxidation and is located approximately 18 Å below the protein surface close to the subunit interface. It is covalently bound to the protein by five cysteine residues and one histidine residue. All Fe atoms of the cluster are tetrahedrally coordinated. Three of the Fe atoms (Fe2, Fe3, and Fe4) build a [3Fe−3S] subsite with a geometry similar to that of a cubane-type [4Fe-4S] cluster. Fe1 is unusually coordinated by a cysteine and a histidine residue and shows nearest Fe−Fe distances of 3.3 Å. The Ni ion is an integral constituent of cluster C and is coordinated by four S atoms. One S ligand originates from a cysteine residue, two are μ_3-S atoms, and one is a μ_2-S atom, which coordinates Ni and Fe1 and completes the square-planar ligand geometry at Ni[8] (Figure 1A). Structures of cluster C from the CODHs of *Rhodospirillum rubrum* (CODH$_{Rr}$) at 2.8 Å

resolution[14] and *Moorella thermoacetica* (CODH$_{Mt}$) at 2.2 and 1.9 Å resolution[15,16] confirmed the positions of the five metal ions but described dissimilar geometries at Ni and Fe1, all of which lack a bridging sulfido ligand between the two metals. Thus, these structures presented cluster C as a cubane [Ni−3Fe−4S] cluster linked to a mononuclear Fe site (Figure 1B−D).

The oxidation of CO at cluster C would involve the temporary binding of CO. The prime candidate for CO binding is the Ni ion, because of its direct accessibility through the substrate channel and its empty apical coordination site.[8] It has been shown that the capacity of Ni ions to bind CO in their +II oxidation state is dependent on the number of significant π-donor ligands and their geometrical arrangement.[19] Fe1 is the presumed hydroxyl-donor ligand in CO$_2$ formation.[20]

In recent studies, we observed various stabilities of the CO oxidizing activity of CODHII$_{Ch}$, which depended on the presence or absence of CO and the reducing agents employed. These

(13) Svetlitchnyi, V.; Dobbek, H.; Meyer-Klaucke, W.; Meins, T.; Thiele, B.; Römer, P.; Huber, R.; Meyer, O. *Proc. Natl. Acad. Sci. U.S.A.* **2004**, *101*, 446−451.

(14) Drennan, C. L.; Heo, J.; Sintchak, M. D.; Schreiter, E.; Ludden, P. W. *Proc. Natl. Acad. Sci. U.S.A.* **2001**, *98*, 11973−11978.
(15) Doukov, T. I.; Iverson, T. M.; Seravalli, J.; Ragsdale, S. W.; Drennan, C. L. *Science* **2002**, *298*, 567−572.
(16) Darnault, C.; Volbeda, A.; Kim, E. J.; Legrand, P.; Vernede, X.; Lindahl, P. A.; Fontecilla-Camps, J. C. *Nat. Struct. Biol.* **2003**, *10*, 271−279.
(17) Doukov, T. I.; Iverson, T. M.; Seravalli, J.; Ragsdale, S. W.; Drennan, C. L. *Science* **2002**, *298*, 567−572.
(18) DeLano, W. L.; DeLano Scientific: San Carlos, CA, 2002.
(19) Macgregor, S. A.; Lu, Z.; Eisenstein, O.; Crabtree, R. H. *Inorg. Chem.* **1994**, *33*, 3616−3618.
(20) DeRose, V. J.; Telser, J.; Anderson, M. E.; Lindahl, P. A.; Hoffman, B. M. *J. Am. Chem. Soc.* **1998**, *120*, 8767−8776.

Table 1. Refinement Statistics[a]

data set	total/unique refl	R_s[b]	resolution (Å)	completeness (%)	$\langle I \rangle/\langle \sigma I \rangle$, overall/last shell	model R/R_{free}-factor[c] (%)	resolution (Å)
N$_2$_Dithio	611670/216577	0.047	20−1.10	98.4	28.5/2.3	12.3/15.2	8−1.10
N$_2$_DTT	585926/205157	0.046	30−1.12	94.1	27.4/2.1	12.0/15.2	8−1.12
CO_DTT	534177/180964	0.067	20−1.15	93.2	25.8/2.3	12.3/15.4	8−1.15
CO_fast	210527/66048	0.074	30−1.64	95.5	11.7/3.1	15.9/19.9	8−1.64

[a] N$_2$_Dithio: CODHII$_{\text{Ch}}$ crystal in the presence of 2 mM dithionite under N$_2$. N$_2$_DTT: CODHII$_{\text{Ch}}$ crystal in the presence of 2 mM DTT under N$_2$. CO_DTT: CODHII$_{\text{Ch}}$ crystal in the presence of 2 mM DTT under CO. CO_fast: CODHII$_{\text{Ch}}$ crystal in the presence of 2 mM DTT and 1 h exposure to CO. CO_fast was measured on a rotating Cu-anode X-ray generator; all other datasets were measured at the synchrotron beamline BW6, DESY, Hamburg. [b] $R_s = \Sigma (I - \langle I \rangle)/\Sigma (I)$; I measured intensity, $\langle I \rangle$ averaged value; the summation is over all measurements. [c] The free R-factor was calculated from 5% of the data, which were removed at random before the refinement was carried out.

observations prompted us to examine the structures of cluster C of CODHII$_{\text{Ch}}$ under these conditions by X-ray crystallography and to determine their corresponding functionality.

Experimental Procedures

Purification and Manipulation of CODHII$_{\text{Ch}}$. *C. hydrogenoformans* Z-2901 (DSM 6008) was grown as described previously with CO as the energy and carbon source.[12] CODHII$_{\text{Ch}}$ was purified and maintained under strict anoxic conditions as detailed before.[12] The gases used for purification, manipulation, and crystallization of CODHII$_{\text{Ch}}$ (N$_2$ and CO) were purified of traces of oxygen by passing over a heated copper catalyst. CO oxidation activity was assayed as described.[12] Protein estimation employed conventional methods[21] with bovine serum albumin as a standard. Purified CODHII$_{\text{Ch}}$ had a specific activity of 14 000 μmol of CO oxidized min^{-1} mg^{-1} of protein at 70 °C, pH 8.0, and 20 mM methyl viologen as electron acceptor.[12]

Stability Testing. The stability of CODHII$_{\text{Ch}}$ was examined in experiments modeling the conditions of crystallization. The assays (1 mL) contained 16 μg of CODHII$_{\text{Ch}}$ in 50 mM HEPES/NaOH (pH 8.0) in the absence or in the presence of 2 mM reducing agent [dithiothreitol (DTT), dithionite, or Ti(III) citrate] under an atmosphere of oxygen-free N$_2$ or oxygen-free CO. The assays were performed at 23 °C in 17-ml tubes fitted with butyl rubber stoppers. Aliquots were removed with time and analyzed for CO-oxidation activity. The presence of traces of oxygen in the stability assays can be excluded, since (a) the assays containing Ti(III) citrate retained violet color during the time of the assays indicating reducing conditions and (b) after addition of the redox-indicator resazurin to the assays the indicator became colorless ($E_h <$ −110 mV).

Crystallization. Crystallization of CODHII$_{\text{Ch}}$ was performed at 23 °C in an anoxic glovebox chamber (model 1024 anaerobic system equipped with plexiglass front window; Forma Scientific, Marietta, Ohio) filled with oxygen-free N$_2$ as described previously.[8] A CODHII$_{\text{Ch}}$ solution (6 μL) containing 16 mg ml^{-1} in 20 mM Tris/HCl (pH 7.5) was mixed with 6 μL of the crystallization solution from the reservoir supplemented with 2 mM DTT or 2 mM dithionite and incubated under oxygen-free N$_2$ or oxygen-free CO in the gas phase of the reservoir. The presence of traces of oxygen during the crystallization can be excluded: the redox-indicator resazurin, which was routinely added to the crystallization solution in the reservoir after the mixing of protein with the crystallization solution in the drop, remained colorless during the crystallization. Depending on the conditions crystals appeared within 1 to 3 days. The dithionite- and DTT-reduced crystals grown under an atmosphere of N$_2$ (N$_2$_Dithio and N$_2$_DTT, respectively, in Table 1) were harvested after 24 h, the DTT-reduced crystals grown under an atmosphere of CO (CO_DTT in Table 1) were harvested 48 h after the set up of the experiments. The DTT-reduced crystals with short exposure time to CO (CO_fast in Table 1) were grown under an atmosphere of N$_2$ for 24 h and finally incubated for 1 h in CO-saturated crystallization solution containing 2 mM DTT before freezing. The

Table 2. Occupancies and *B*-value of Selected Atoms[a]

atom	N$_2$_Dithio Occ/*B*-value	N$_2$_DTT Occ/ *B*-value	CO_DTT Occ/ *B*-value	CO_fast Occ/ *B*-value
Ni	0.93/11.24	0.93/12.3	0.6/12.8	0.8/15.0
Fe1	0.80/10.98	0.90/12.30	0.6/13.4	0.8/16.36
Fe1B	0.10/9.16	0.0	0.3/13.2	0.0
μ_2-S	0.83/13.9	0.83/15.34	0.0	0.8/17.3

[a] Occupancies for individual atoms of cluster C have been adjusted during refinement to give similar *B*-values for neighboring atoms. Fe1 refers to the highly populated position, and Fe1B, to the alternative position found for Fe1.

crystals in the corresponding reservoir solution were supplemented with 5% (v/v) glycerol, shock frozen, and stored in liquid nitrogen.

Structure Solution and Refinement. Diffraction data were collected at 100 K on a beamline BW6 (DESY, Hamburg, Germany) or a rotating Cu-anode X-ray generator equipped with a MarResearch image plate. All synchrotron datasets were collected on a MarResearch CCD detector at a wavelength of 1.05 Å. Data were indexed, integrated, and scaled with the XDS program package.[22] The structures were refined using CNS[23] and SHELX[24] (when $d_{\text{min}} <$ 1.2 Å using individual anisotropic *B*-value refinement). Model building has been carried out using MAIN[25] and XtalView[26] for modeling of disorder.

Results and Discussion

Effect of Anoxic Incubation Conditions on the Activity of CODHII$_{\text{Ch}}$. This study started from the observation that the conditions applied for crystallization of CODHII$_{\text{Ch}}$ have an effect on the CO-oxidizing activity as well as on the structure of cluster C. Therefore, we became interested to examine the CO-oxidation activity of the enzyme under different conditions with time (Figure 2).

In the presence of the reducing agents dithionite and Ti(III) citrate, CODHII$_{\text{Ch}}$ was completely stable for at least 100 hours under N$_2$ but slowly inactivated when N$_2$ was replaced by CO. In the presence of DTT or in the absence of reductants, CODHII$_{\text{Ch}}$ was slowly inactivated under N$_2$ but rapidly inactivated under CO (Figure 2). The highest rate of inactivation was observed when the enzyme was incubated under CO in the absence of reducing agents. The data indicate the formation of nonfunctional species of CODHII$_{\text{Ch}}$ under strictly anoxic conditions.

(21) Bradford, M. M. *Anal. Biochem.* **1976**, *72*, 248−254.

(22) Kabsch, W. *J. Appl. Crystallogr.* **1988**, *21*, 67−71.
(23) Brünger, A. T.; Adams, P. D.; Clore, G. M.; Delano, W. L.; Gros, P.; Grosse Kunstleve, R. W.; Jiang, J. S.; Kuszewski, J.; Nilges, M.; Pannu, N. S.; Read, R. J.; Rice, L. M.; Simonson, T.; Warren, G. L. *Acta Crystallogr., Sect. D* **1998**, *54*, 905−921.
(24) Sheldrick, G. M.; Schneider, T. R. *Methods Enzymol.* **1997**, *277*, 319−343.
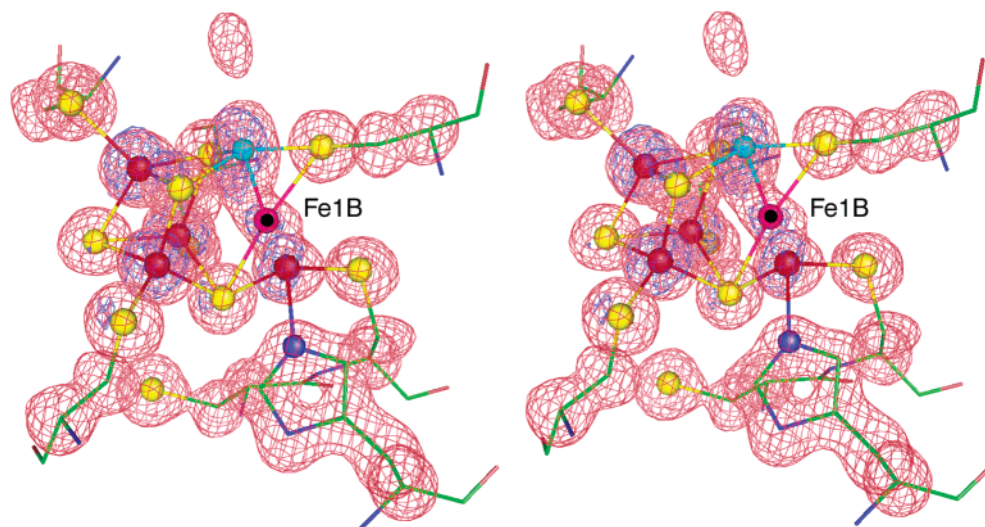(25) Turk, D. TU München: München, 1992.
(26) McRee, D. E. *Practical Protein Crystallography*; Academic Press Inc.: San Diego, CA, 1993.
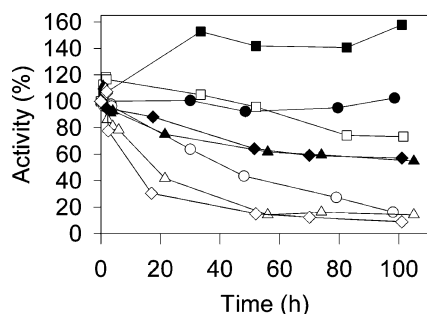
Figure 2. Stability of CODHII$_{Ch}$ under an atmosphere of N$_2$ or CO. CODHII$_{Ch}$ (16 μg ml^{-1}) was incubated as described in Experimental Procedures in the presence of 2 mM dithionite (■, □), 2 mM Ti(III) citrate (●, ○), or 2 mM DTT (▲, △) as well as without reducing agents (◆, ◇) under an atmosphere of N$_2$ (solid symbols) or CO (open symbols) at 23 °C. CO-oxidation activity was assayed at 70 °C; 100% of activity corresponds to 14 000 μmol of CO oxidized min^{-1} mg^{-1} of protein.

Structure of Cluster C in DTT-Reduced CODHII$_{Ch}$ under CO. We have determined the structure of CODHII$_{Ch}$ crystallized in the presence of DTT under CO atmosphere (CO_DTT) (Figure 3). This is the inactivated CODHII$_{Ch}$ species (Figure 2). The high-resolution datasets were recorded to 1.15 Å (Table 1), allowing us to resolve mixed states and the corresponding multiple conformations. The refined structure has R-factors of 12.3%/R_{free}: 15.4%.

The structure shows a well ordered [3Fe−3S] cluster (Figure 3), which, unlike the enzyme crystallized in the absence of CO (Figure 5), shows neither an alternative position for Fe2 nor dual conformations for Cys526. The [Fe1−μ_2S−Ni] subsite is strongly affected by crystallization in the presence of CO, as it shows a reduced occupancy of Ni, two only weakly occupied positions for Fe1, and the absence of the μ_2-S ligand (Figure 3). Occupancies suggest that Fe1 and Ni have both occupancies of around 60%, while approximately 30% of the Fe is found in the alternative position Fe1B (Table 2). The distance of 2.0 Å between Ni and the alternative position of Fe1 (Fe1B in Figure 3) is unusually short, and the position of Fe1B may only be occupied in the absence of Ni, which would be in agreement with the similar occupancies found for Ni and Fe1.
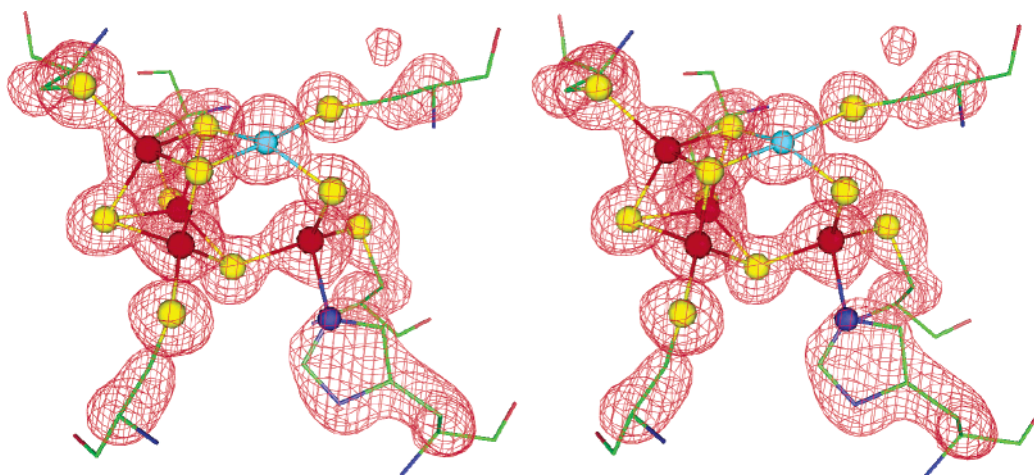
Residual density at the apical coordination site of Ni is considerably stronger than in the dithionite reduced state reported previously [8] and may indicate a bound ligand at the Ni, which might be CO. The treatment of CODHII$_{Ch}$ under these conditions has led to a mixture of approximately 80% nonfunctional and 20% functional enzyme species in the crystals. Therefore, we do not attribute any functional significance to this residual density. The structures of the [Ni−4Fe−4S] clusters reported by Drennan et al.,[14] Doukov et al.,[17] and Darnault et al.[16] refer to CODHs which apparently have been exposed to CO. As these, the CO_DTT form of CODHII$_{Ch}$ accommodates a [Ni−4Fe−4S] cluster, does not contain a μ_2-S ligand, and shows additional density at the apical Ni position (Figure 3). As the CO_DTT form of CODHII$_{Ch}$ is composed of mostly inactive enzyme (Figure 2), we conclude that the [Ni−4Fe−4S] form of cluster C represents a nonfunctional state.

No loss of atoms in clusters B and D is detectable which remain in the classical cubane-type [4Fe−4S] cluster geometry.[8]

Structure of Cluster C in DTT-Reduced State after 1 h of Exposure to CO. The brown color of CODHII$_{Ch}$ crystals grown with DTT under N$_2$ is immediately bleached after the transfer of the crystals to crystallization solution saturated with CO. This indicates the reduction of the protein metal clusters in the crystals and is in accordance with the previously observed fast reduction of oxidized CODHII$_{Ch}$ after the addition of CO.[12] A crystal grown in the presence of DTT has been exposed to CO for approximately 1 h (CO_fast). A diffraction dataset to 1.64 Å resolution has been collected, and the corresponding structure has been refined to an R-factor of 15.9%/R_{free}: 19.9% (Table 1) with anisotropic B-values for Ni, Fe, and S.

Electron densities at the μ_2-S ligand indicate a high occupancy for this ligand (Figure 4 and Table 2). This density was absent in CO_DTT CODHII$_{Ch}$ (Figure 3). There is no density that can be attributed to a CO ligand at the Ni-ion. The CO_fast state represents the functional [Ni−4Fe−5S] cluster in its CO-reduced state, which contains the μ_2-S ligand. The CO-reduced [Ni−4Fe−5S] cluster (Figure 4) is converted to the [Ni−4Fe−4S]

Figure 3. Stereo presentation of cluster C in the DTT-reduced state under CO (CO_DTT). An $F_{obsd} - F_{calcd}$ omit electron density map contoured at a 4σ level is depicted in red. Omitted from the calculation of the F_{calcd}-part were all atoms of cluster C including their direct ligands. Side chains coordinating cluster C were omitted starting from their Cα-atoms as in Figures 4 to 6. An anomalous difference Fourier map contoured at 5σ is shown in blue. The conformations/positions with minor occupancy are marked by a black dot, as in Figures 5 and 6. Fe is shown in red, S, in yellow, Ni, in cyan, N, in blue, and C, in green.

Figure 4. Stereo presentation of cluster C in the DTT-reduced state after short exposure to CO (CO_fast). An $F_{obsd} - F_{calcd}$ omit electron density map is depicted in red. Omitted from the calculation of the F_{calcd}-part were all atoms of cluster C including their direct ligands. Side chains coordinating cluster C were omitted starting from their Cα-atoms as in Figures 3−6.
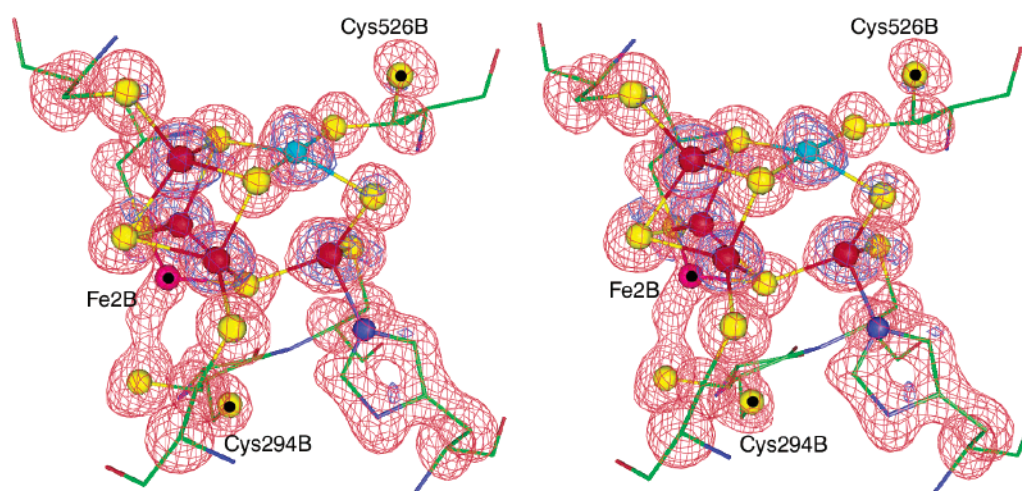
Figure 5. Stereo presentation of cluster C in the DTT-reduced state under N_2 (N_2_DTT). An $F_{obsd} - F_{calcd}$ omit electron density map is depicted in red. Omitted from the calculation of the F_{calcd}-part were all atoms of cluster C including their direct ligands. An anomalous difference Fourier map contoured at 3σ is shown in blue.

cluster only by the prolonged exposure to CO (Figure 3), resulting in the inactivation of the enzyme (Figure 2).

Structure of Cluster C in DTT-Reduced CODHII$_{Ch}$ under N_2. The crystal structure of CODHII$_{Ch}$ treated with DTT under N_2 atmosphere (N_2_DTT) was refined to a resolution of 1.12 Å with R-factors of 12.0%/R_{free}: 15.2%. (Tab.1). The cluster is in general very similar to the dithionite-reduced [Ni−4Fe−5S] cluster previously reported.[8]

A difference is that alternative conformations at Cys526, Cys294, and Fe2 are observed (Figure 5). Cys526 is the only protein ligand at the Ni-ion and shows dual conformations. Given the observation that CODHs are active in a low redox regime ($E_o' < -380$mV),[27] the conformation of cluster C in the N_2_DTT state does presumably not reflect the physiologically active state. Approximately 75% of CO-oxidizing activity remained after treatment of CODHII$_{Ch}$ for 24 h with DTT under CO (Figure 2). Considering the structure, this may reflect a partial loss of Fe2 (Figure 5).

Structure of CODHII$_{Ch}$ in the Dithionite-Reduced State under N_2. Figure 6 shows CODHII$_{Ch}$ after reduction with dithionite under N_2 (N_2_Dithio CODHII$_{Ch}$). The specific CO oxidation activity of the N_2_Dithio CODHII$_{Ch}$ in dissolved

crystals was 99 to 104% of the specific activity of protein used for crystallization; it therefore, contains cluster C in the fully functional state. The structure of cluster C in N_2_Dithio CODHII$_{Ch}$ was solved at atomic resolution using synchrotron radiation (Figure 6). A data set was collected to a resolution of $d_{min} = 1.10$ Å (Table 1). The refined structure has R-factors of 12.3%/R_{free}: 15.2%.

The structure reveals the [Ni−4Fe−5S] cluster and is essentially the same as described earlier at lower resolution.[8] Features that have not been detected before are the weakly occupied alternative positions of two Fe atoms and two cysteine residues (Figure 6). Fe1 adopts two positions lying approximately 1.2 Å apart, with the main contribution originating from the tetrahedrally coordinated species with four different ligands. The two alternative positions of both Fe ions (Fe1 and Fe2) are identified on the basis of their anomalous absorption (data not shown). Thus, these minor contributions cannot be interpreted as small ligands at the corresponding Fe-positions.

It would be attractive to assume an O atom as the bridging ligand between Ni and Fe1 serving as the nucleophile that

(27) Heo, J.; Halbleib, C. M.; Ludden, P. W. *Proc. Natl. Acad. Sci. U.S.A.* **2001**, *98*, 7690−7693.
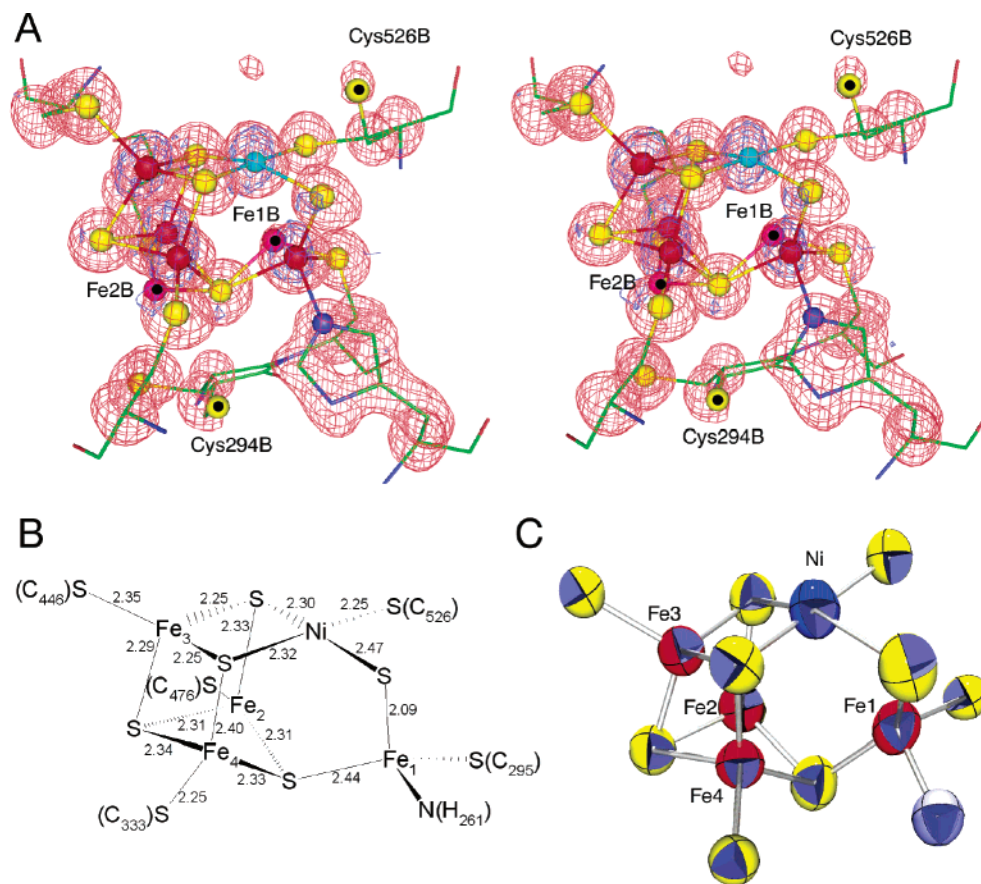
Figure 6. Cluster C in the dithionite-reduced state under N_2 (N_2_Dithio). (A) Stereo representation of cluster C. An $F_{obsd} - F_{calcd}$ omit electron density map is depicted in red. Omitted from the calculation of the F_{calcd}-part were all atoms of cluster C including their direct ligands. An anomalous difference Fourier map contoured at 3σ is depicted in blue. (B) Observed bond distances of the [Ni−4Fe−5S] cluster. (C) ORTEP presentation of the [Ni−4Fe−5S] cluster and atoms directly coordinating the cluster. The ellipsoid probability is 30%. Part C has been created using the program ORTEP-3.[28]

attacks the Ni-bound CO. To check this model, anomalous difference Fourier syntheses were calculated using the datasets N_2_Dithio and N_2_DTT (Table 1). They display comparable signals for most of the S atoms of the structure including the Ni−Fe1 bridging ligand (Figures 5 and 6). Because of the very weak anomalous scattering of O at a wavelength of 1.05 Å (Table 1), the anomalous scattering properties exclude the interpretation of the bridging ligand as an oxygen atom. The fit into the electron density, the anomalous scattering, and the observed distances to the two metal atoms further support the interpretation of this atom being a bridging μ_2-S ligand.

The atomic resolution structures of CODHII$_{Ch}$ resolve the existing controversy regarding the direct Ni coordination environment of cluster C. From the described structures and their corresponding activities, we conclude that the activity of a CODHII$_{Ch}$ preparation is governed by the presence of the μ_2-S ligand in cluster C. This identifies the [Ni−4Fe−5S] cluster as a functional species and the [Ni−4Fe−4S] cluster as a non-functional species. Although the reactions leading to the removal of the μ_2-S from the [Ni−4Fe−5S] cluster still remain to be elucidated, it is tempting to assume that CO reacts with a μ_2-S^{2-} to form carbonyl sulfide (COS).

We cannot conclude from our results which aspect of the μ_2-S ligand is important for the catalytic CO oxidation. However, a role of the μ_2-S ligand in the stabilization of the [Fe1−μ_2S−Ni] subsite would be in agreement with the partial loss of both metals as observed in the CO_DTT state (Figure 3 and Table 2) Furthermore, we could neither observe a bound CO molecule at the functional [Ni−4Fe−5S] cluster nor detect the presence of an OH-ligand in any oxidation state. To define these important subjects for the mechanism of a CO oxidation at cluster C, further experiments will be necessary.

(28) Barnes, C. L. *J. Appl. Crystallogr.* **1997**, *30*, 568−568.

JA037776V